ELSEVIER

Postharvest Biology and Technology 20 (2000) 175–184

Postharvest Biology and Technology

www.elsevier.com/locate/postharvbio

Comparison of reflectance, interactance and transmission modes of visible-near infrared spectroscopy for measuring internal properties of kiwifruit (*Actinidia chinensis*)

P.N. Schaare *, D.G. Fraser

Technnology Development Group, HortResearch, Private Bag 3123, Hamilton, New Zealand

Received 18 November 1999; accepted 6 June 2000

Abstract

Three modes of visible-near infrared spectroscopic measurement (reflectance, interactance and transmission) were compared for their ability to non-destructively estimate harvest soluble solids content (SSC), density and internal flesh colour of the yellow-fleshed kiwifruit *Actinidia chinensis*. Interactance mode spectra provided the most accurate estimates of SSC, density and flesh colour. SSC was predicted with a standard error of prediction (SEP) of $\pm 0.80°$ Brix and with correlation coefficient R^2 of 0.93. Whole-fruit densities were predicted with an SEP of ± 3.6 kg m^{-3} and with an R^2 of 0.74. Internal flesh hue angle was predicted with an SEP of $\pm 1.6°$ and with an R^2 of 0.82.

Keywords: NIR; Non-destructive test; Kiwifruit; Fruit quality; Soluble-solids content; Density; Flesh colour

1. Introduction

Near infrared spectroscopy has been shown to provide rapid and non-destructive measurements of internal properties such as soluble solids concentration (SSC) and dry matter for many fruits and vegetables (Dull et al., 1989; Kawano et al., 1992; Bellon et al., 1993; Kawano et al., 1993; Kawano, 1994; Abbott et al., 1997), including kiwifruit (Jordan et al., 1997; McGlone and Kawano, 1998). However, application of the technique varies. Some workers use reflectance mode, where the field of view of the light detector includes parts of the fruit surface directly illuminated by the source (Mowat and Poole, 1997). Others use transmission mode, where the fruit surface viewed by the detector is diametrically opposite to the illuminated surface (Kawano et al., 1993; Miyamoto and Yoshinobu, 1995; Greensil and Newman, 1999). Others use interactance mode, where the field of view of the detector is separated from the illuminated surface by a light seal in contact with the fruit surface (Dull et al., 1989; McGlone and Kawano, 1998; Osborne et al., 1998).

The relative merits of each of the different modes of near infrared spectroscopy have become

* Tel.: +64-7-8584760; fax: +64-7-8584705.
E-mail address: pschaare@hort.cri.nz (P.N. Schaare).

0925-5214/00/$ - see front matter
PII: S0925-5214(00)00130-7

of commercial importance with the application of the technique to on-line grading of fruit for internal qualities (Miyamoto et al., 1997; Schmilovitch et al., 1997; Greensil and Newman, 1999). Reflectance mode measurements are the easiest to obtain because they require no contact with the fruit and light levels are relatively high. However, calibrations may be susceptible to variations in superficial or surface properties of the fruit. Transmission mode measurements may also be made without contacting the fruit and may be less susceptible to surface properties and better for detecting internal disorders than reflectance mode measurements. However, the amount of light penetrating the fruit is often very small, making it difficult to obtain accurate transmission measurements at grading line speeds, particularly in conditions of high ambient light levels. Interactance mode provides a compromise between reflection and transmission modes in each of these characteristics, but obtaining a light seal may be problematic at the high conveyor speeds used in modern fruit grading systems.

Despite these uncertainties there have been few studies that directly compare the merits of the different measurement modes. This study aims to quantify the relative accuracy of each mode for estimating properties of the yellow-fleshed kiwifruit *Actinidia chinensis*.

We compare the accuracy of the different spectroscopic modes in estimating the harvest-time soluble solids content (SSC), density and flesh hue of *Actinidia chinensis*. Harvest-time SSC is an indicator of fruit maturity, as the SSC of *Actinidia* rises as starch reserves in the berry are converted to sugars during maturation. Flesh hue is an important quality parameter for *Actinidia chinensis* as its unique golden colour at maturity is a primary factor in the appeal of the fruit to the consumer, but fruit harvested too soon retain their immature green flesh colour. Harvest-time density of the common kiwifruit cultivar 'Hayward' (*Actinidia deliciosa*) is correlated with soluble solids content of fully ripened fruit (Asami et al., 1988), which is used by the New Zealand kiwifruit industry as an indicator of maturity. Harvest-time density may provide an indicator of maturity for *Actinidia chinensis* and, while such a relationship has not been verified, density measurements were included in this experiment for interest.

2. Method

Fruit for this study were obtained from four orchards spread through the Northland, Waikato and Bay of Plenty regions of the North Island of New Zealand. Fifty fruit were harvested weekly from each orchard for a period from ≈ 4 weeks preceding to 1 week following normal harvest. Fruit were hand-picked from random locations on vines, transported to the laboratory and stored at room temperature before assessment the following day. Transmission, interactance and reflectance spectra were collected from over 1000 fruit over a 7 week period. For most fruit single reflectance, transmission and interactance spectra were measured from random positions on the circumference. All fruit were also assessed immediately after spectrum collections for SSC, density and flesh hue. For a subset of 50 fruit a second spectrum was recorded from random positions on the circumference, and density, SSC and hue measurements were replicated.

The apparatus used for reflectance measurements is shown in schematic form in Fig. 1(a). For reflectance measurements fruit were illuminated by a single 50 W tungsten filament lamp powered by a DC regulated supply. The detector was a solid state spectrometer (Zeiss MMS-1 Spectrometer, Carl Zeiss Jena Gmbh, Jena, Germany) that uses a silicon photodiode array. Light entered the spectrometer through a 500 μm diameter optical fibre bundle. The spectrometer provided 15-bit intensity measurements at 256 wavelengths from 300 to 1100 nm with 3.3 nm resolution and ≈ 10 nm bandwidth. The acceptance angle of the optical fibre was 11.5°, so that at the working distance of ≈ 45 mm from the fruit surface the field of view was a circle of 18 mm diameter. A block of white polytetrafluroethylene (PTFE) measuring 80 $mm^2 \times 40$ mm thick was located in place of the fruit as a reference surface. Before each batch of 50 fruit from an orchard was assessed, both a reference spec-

trum and a dark spectrum (obtained by blocking the aperture to the optical fibre) were recorded. The integration period for reflectance spectra was 15 ms.

Fig. 1(b) depicts the apparatus used to measure transmission spectra. A constant voltage 230 VAC regulator powered a 650 W tungsten halogen lamp. Fruit were positioned in a 46×34 mm ovoid hole in a black foam (Skellerup Starthene, Skellerup Industries Ltd., Christchurch, New Zealand) light seal over the lamp. The high power of the lamp required the lamp to be turned on from a standby 'warm' state for only a few seconds before each measurement to avoid overheating the light seal and fruit. Reference spectra were obtained by measuring transmission spectra through an 80 $mm^2 \times 52$ mm thick PTFE block. Reference and dark spectra were recorded before assessing the 50 fruit batch from each orchard. Integration periods for transmission spectra were varied between 1000 ms at the beginning and 100 ms at the end of the experiment as fruit became increasingly transparent with advancing maturity. The same spectrometer was used for both transmission and reflection measurements.

The configuration for measurement of interactance spectra is shown in Fig. 1(c). Fruit were placed on a rubber seal and illuminated from below by a single 12 V, 50 W, tungsten–halogen lamp powered by a regulated DC supply. The interactance system used an identical spectrometer to that used for the reflection and transmission measurements. Light passing through the fruit and emerging inside the light seal was reflected onto the entrance aperture of the fibre by a 45° mirror. The acceptance angle of the optical fibre is 11.5°, so that at a distance of ≈ 18 mm from the fruit surface the field of view was a circle of 7 mm diameter. The reference body for interactance measurements was an 80 $mm^2 \times 40$ mm thick block of white PTFE shaded by a hood of 10 mm-thick black PTFE. The white reference surface was placed against the light seal shown in Fig. 1(c) to make a reference measurement. The spectrometer integration period for interactance spectra was 100 ms.

After reflectance, transmission and interactance spectra had been obtained, fruit density was measured using a buoyancy method. Flesh hue angle was measured by removing two 1 mm slices of skin from a random position on the fruit equator and measuring the colour co-ordinates of the exposed section of flesh, $\approx 10 \times 15$ mm, with a colour meter (Minolta Color Meter CR200, Minolta Co. Ltd., Osaka, Japan). Finally, the SSC of each fruit was measured. 10 mm-thick caps were sliced from both stem and calyx ends of the fruit, the °Brix of juice squeezed from each end cap was measured using a refractometer (Palette PR-100 Digital Refractometer, Atago Co Ltd., Tokyo, Japan) and the two readings were averaged to give an SSC estimate for the entire fruit.

The repeatability of SSC, density and hue angle measurements was measured in one batch of 50

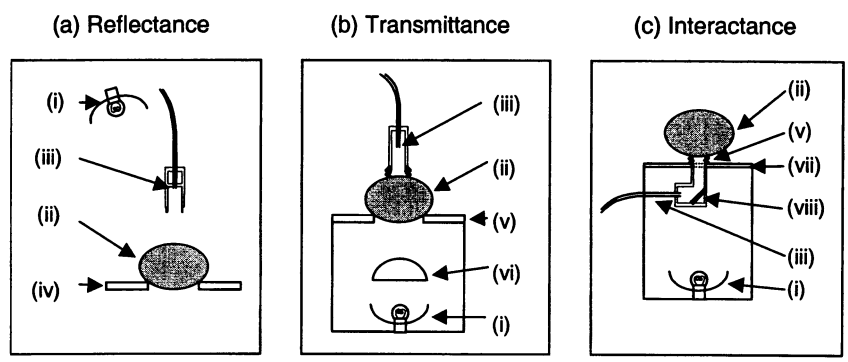

Fig. 1. The apparatus used for measuring (a) reflectance; (b) transmittance; and (c) interactance spectra of kiwifruit, showing (i) the light source; (ii) fruit; (iii) fibre bundle aperture; (iv) black foam holder; (v) light seal; (vi) condensing lens; (vii) glass top; and (viii) mirror.

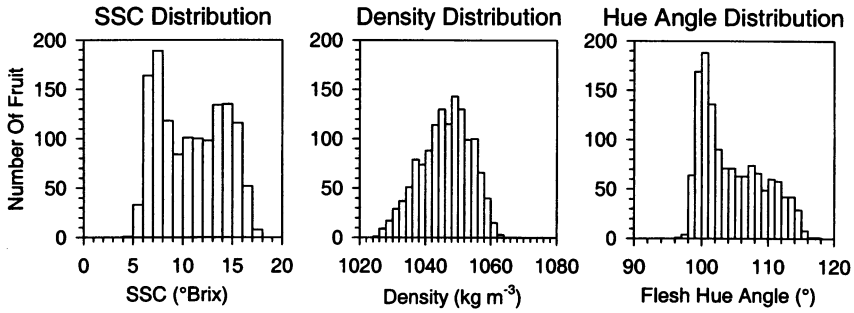

Fig. 2. Distribution of SSC, whole fruit density and flesh hue angle in the sample.

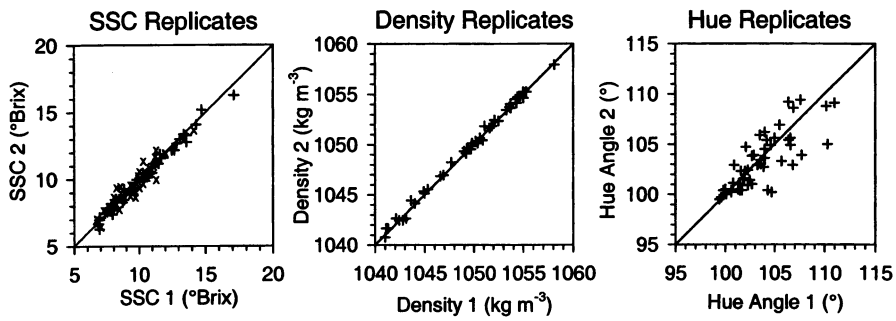

Fig. 3. Replicate measurements within fruit of SSC (from the stem (+) and calyx (×) ends of the fruit), whole fruit density and flesh hue angle.

fruit. SSC repeatability was assessed by bisecting the stem end and calyx end slices and making separate measurements of the SSC of the halves of each slice. Fruit density measurements were also repeated on this sample of fruit, and replicate flesh hue colour measurements were taken from opposite sides of the fruit.

3. Results

Fruit SSC ranged from approximately 5°Brix early in the season to 17°Brix for mature fruit. Fig. 2(a) shows the distribution of SSC for all fruit in the experiment. The bimodal distribution of SSC results from the relatively static sugar levels at early harvests and the subsequently rapid transition from low to high values during fruit ripening. Whole-fruit densities ranged from 1025 to 1063 kg m^{-3} as shown in Fig. 2(b). Flesh hue angle varied from 118° (mid-green) on immature fruit down to 97° (greenish yellow) for mature fruit.

The repeatability of SSC, density and hue angle measurements was measured in 50 fruit. Fig. 3 demonstrates that the replicate measurements of both SSC and density showed good repeatability, although a small bias is evident in the repeated density measurements. However, repeatability in flesh hue angle measurements was comparatively poor.

However, there was a systematic difference in SSC between the ends of the fruit. Fig. 4 shows the difference in SSC between the stem and calyx ends as a function of the average of the two SSC values. In immature fruit with low SSC there was little systematic difference in SSC between the ends of the fruit. However, as the fruit mature and SSC increases an SSC gradient developed between the ends of the fruit so that average SSC at the stem end was over 2°Brix higher than at the calyx end. There is also some suggestion in Fig. 4 that the SSC gradient began to decline as the fruit matured further.

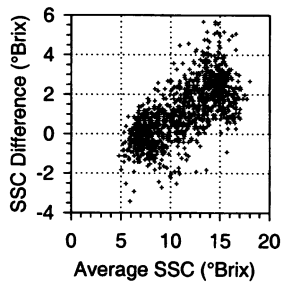

Fig. 4. The difference in SSC between the stem and calyx ends of the fruit, as a function of the average SSC.

Fig. 5 shows typical transmission, interactance and reflectance spectra. The greatest variation in spectra was observed in transmittance mode, where mean intensity increased as fruit ripened. For analysis, spectra were truncated where the estimated signal to noise ratio dropped below unity. Thus reflectance spectra ranged from 450 to 1100 nm, interactance spectra from 520 to 1100 nm and transmission spectra from 690 to 1080 nm.

A systematic analysis of the standard error of prediction (SEP) (Fearn, 1996) was used to select an optimal calibration procedure for estimating SSC. Calibrations were calculated using the Matlab Chemometrics Toolbox (Matlab, The MathWorks Inc, Natick, MA). The data set was divided randomly into calibration and prediction sets of ≈ 500 samples each. Spectra were normalised using the PTFE references. Twelve spectrum pre-processing transformations, listed in Table 1, were combined with four computation algorithms to generate calibrations. The computation algorithms were: Classical Least Squares (CLS), Inverse Least Squares (ILS), Principle Component Regression (PCR) and Partial Least Squares (PLS). PCR and PLS were applied using 2, 4, 6, 8, 10, 15, 20, 30 and 40 terms. The resulting 240 calibrations for each spectral mode (reflectance, interactance and transmission) were ranked by SEP and their bias and SEP were compared following the method of Fearn (1996). Table 2 lists the calibration algorithm with the lowest SEP (the 'best' algorithm) for each spectral mode along with the algorithms that had bias and SEP not significantly greater than the best algorithm. Where two or more algorithms differed only by the number of PLS or PCR terms used, only that with lowest SEP is listed. Fig. 6 shows the best calibrations between actual and predicted SSC values for each spectral mode.

The method of Fearn (1996) was also used to compare best SSC calibrations between spectral modes. The best interactance mode calibration had a significantly lower SEP ($P < 0.05$) than the transmission mode calibration, which was significantly better in turn than the best reflectance calibration.

Calibrations for whole fruit density were derived following the same procedures as used for deriving SSC calibrations. Table 3 presents the optimal calibration algorithms and results determined for each of the spectral acquisition modes for density, and Fig. 7 shows the relationship between actual and predicted density values calculated from each of the calibrations described in Table 3. Again, interactance spectra provided a

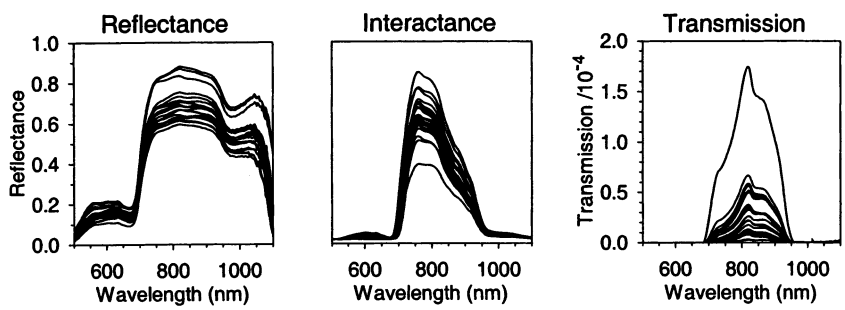

Fig. 5. Typical reflectance interactance, and transmission spectra. The vertical transmission scale is only approximate and the vertical interactance axis shows raw intensity on an arbitrary scale.

Table 1
Pre-calibration transformations applied to spectra[a]

Transform	Description
NONE	$I'_i = I_i$, $I = 1 \ldots n_p$
AREA	Scale all spectra to unity area, using $I'_i = I_i/\Sigma I_j$, $j = 1 \ldots 256$, $i = 1 \ldots n_p$
SMOOTH	Apply simple 5-point smoothing to spectra using $I'_i = (I_I + I_{i+1} + I_{i+2} + I_{i+3} + I_{i+4})/5$, $i = 1 \ldots n_p - 4$
ABS	Apply the absorbance transformation, $I'_i = -\log(1/I_i)$, $i = 1 \ldots n_p$
D1	First smooth using SMOOTH then calculate first differential, using $I'_i = (I_{I+1} - I_i)$, $I = 1 \ldots n_p - 1$
D2	Calculate second differential, using D1 followed by SMOOTH, then $I^{\circ}_j = (I_{j+1} - I_j)$, $j = 1 \ldots n_p - 2$
MAX	Scale all spectra to unity maximum height, using $I'_i = I_i/\max(I_j)$, $j = 1 \ldots n_p$, $i = 1 \ldots n_p$
MSC	Apply multiplicative scatter correction (Geladi et al., 1985) by calculating the average spectrum and then adjusting the slope and offset of each individual spectrum to bring it as close as possible to the average.
SNV	Apply the standard normal variate transformation (Barnes et al., 1989) by shifting and scaling each spectrum to have zero mean and unity variance.
NSD	Calculate the normalised second derivative transformation (Norris, 1997) by first applying the D2 transformation then normalising the area to unity using $I'_i = I_i/\Sigma$ abs(I_j), $j = 1 \ldots n_p$, $i = 1 \ldots n_p$
ABSD1	Calculate the first differential of the absorbance spectrum by applying first the ABS then the D1 transform.
ABSD2	Calculate the second differential of the absorbance spectrum by applying first the ABS then the D2 transform.

[a] n_p is the number of data points in the spectrum.

calibration with a significantly lower SEP ($P < 0.05$) than transmission spectra, with reflectance mode providing the least accurate calibration.

Calibrations for flesh hue angle followed the same procedure as those for SSC and density. Table 4 shows the optimal calibration algorithms and calibration results, and Fig. 8 the corresponding relationships between measured and predicted flesh hue. The best calibration derived from interactance spectra had a significantly lower SEP that those from transmission and reflectance spectra, which were not significantly different.

4. Discussion

The spectra in Fig. 5 demonstrate the differences between the spectral modes. Interactance spectra have general characteristics intermediate between reflectance and transmission spectra. The most apparent difference between reflection and transmission is the spectral range — reflected light could be detected across the range of our spectrometer, while transmitted light was limited to a range of 700–950 nm. Also apparent is the wide range in amplitude of the transmission spectra. Over the 1350 fruit tested, the transmission maximum varied by a factor of 188, from a minimum with large immature fruit to a maximum with small, ripe fruit. The predominant features in the reflectance spectra are the strong absorption troughs at 680 and 970 nm attributed to chlorophyll and water, respectively. Distinct absorption features are evident in the transmission spectra at 730 and 830 nm. It appears that the peak transmission wavelength for interactance spectra, around 760 nm, may differ from the peak for reflectance and interactance spectra, which occurs at 820 nm, but the vertical scale for interactance spectra has not been corrected for instrument response.

While all spectral modes produced good predictions of SSC, density and flesh hue in *A. chinensis*, interactance mode produced the best models in each case. It might be expected that transmission mode, because it is less affected by surface properties than reflectance and interactance modes, should have provided the best estimates of fruit internal properties. Interactance mode may be viewed as intermediary between reflectance and transmission modes in terms of the relative contributions of surface and internal properties to measured spectra and so one might expect the accuracy of interactance calibrations to also be intermediate between those of reflection and transmission calibrations. However, in transmission mode the amount of light penetrating the fruit was very small and resulted in a reduced

signal to noise ratio for transmission spectra compared to those obtained for interactance and reflectance modes. The use of more intense light sources or a more sensitive spectrometer may have increased signal to noise levels and improved transmission mode calibrations.

While the contribution of errors in calibration data to the final SEP is difficult to estimate, the data presented in Fig. 4 suggest that the high SSC gradient along the fruit may contribute significantly to the SEP of the SSC calibrations listed in Table 2. When the average SSC was 15°Brix the average difference in SSC between the two end caps was 2.6°Brix. Using the average SSC to

Table 2
Optimal algorithms and calibration results for estimating soluble solids content of *A. chinensis*[a]

Spectral acquisition mode	Optimal calibration algorithm(s)	Calibration results	
		R^2_P	SEP (°Brix)
Reflectance	**NSD:PLS(30)**, D2:PLS(30), Smooth:PLS(30), D1:PLS(40)	0.86	1.18
Interactance	**NSD:PLS(20)**, NSD:PCR(40), Area:PLS(30)	0.93	0.80
Transmission	NSD:PLS(10), **NSD:PCR(20)**	0.89	1.01.

[a] Algorithms providing the lowest SEP are shown in bold typeface, and those that could not be distinguished from the best on the basis of Bias or SEP (see text) are also listed. Numbers in brackets indicate terms used in PLS or PCR.

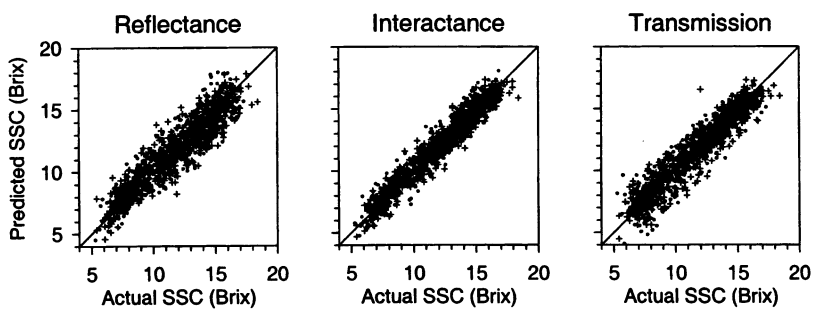

Fig. 6. Comparison of predicted to actual SSC content for the three different spectral modes. Calibration samples are indicated by + and validation data by ●. Some vertical axis labels have been omitted for clarity.

Table 3
Optimal calibrations for predicting whole fruit density of *A. chinensis*[a]

Spectral acquisition mode	Optimal calibration algorithm(s)	Calibration results	
		R^2_P	SEP (kg m^{-3})
Reflectance	**MSC:PLS(20)**, Area:PLS(20)	0.59	4.5
Interactance	**Area:PLS(30)**, Max:PLS(30),Max:PLS(30), Area:PCR(40), MSC:PCR(40)	0.74	3.6
Transmission	**Area:PLS(15)**, Area:PCR(30)	0.55	4.8

[a] Algorithms providing the lowest SEP are shown in bold typeface, and those that could not be distinguished from the best on the basis of Bias or SEP (see text) are also listed. Numbers in brackets indicate terms used in PLS or PCR.

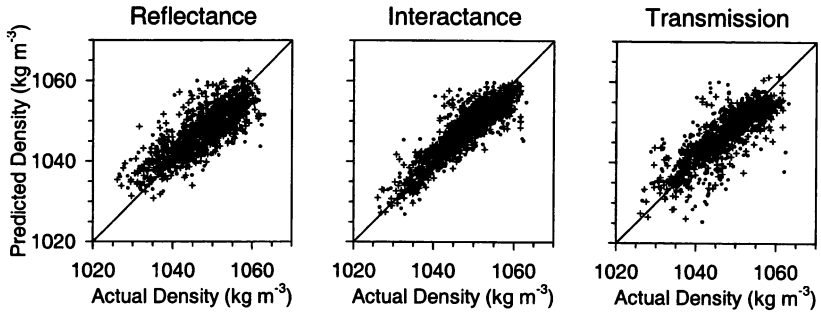

Fig. 7. Comparison of predicted to actual whole fruit density for the three different spectral modes. Calibration samples are indicated by + and validation data by ●. Some vertical axis labels have been omitted for clarity.

Table 4
Optimal calibrations for predicting flesh hue angle of *A. chinensis*[a]

Spectral acquisition mode	Optimal calibration algorithm(s)	Calibration results	
		R^2_P	SEP (Degrees)
Reflectance	**SNV:PLS(30),** MSC:PLS(30), Area:PLS(30), Max:PLS(30)	0.76	1.88
Interactance	**Max:PLS(30),** Area:PLS(30), MSC:PLS(30), SNV:PLS(20)	0.82	1.63
Transmission	**Area:PLS**(8)	0.74	1.95

[a] Algorithms providing the lowest SEP are shown in bold typeface, and those that could not be distinguished from the best on the basis of Bias or SEP (see text) are also listed. Numbers in brackets indicate terms used in PLS.

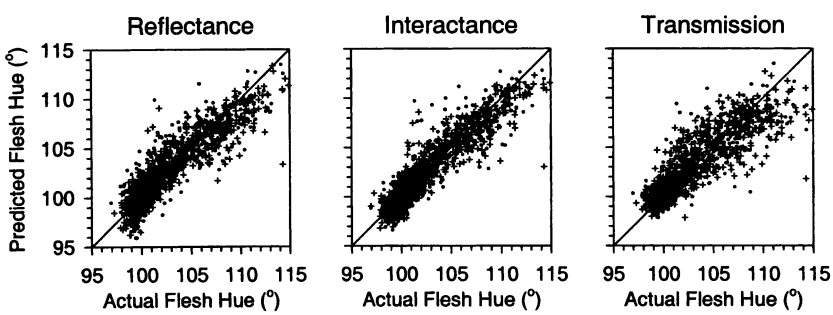

Fig. 8. Comparison of predicted to actual flesh hue angle for the three different spectral modes. Calibration samples are indicated by + and validation data by ●. Some vertical axis labels have been omitted for clarity.

estimate the SSC at the equator of the fruit assumes that the gradient of SSC along the fruit is linear and that spectral measurements were taken at the exact midpoint of the fruit, and in practice both assumptions are only approximate.

The SEP of 0.80°Brix obtained for the interactance calibration of SSC may seem high compared to those reported by others working with kiwifruit (e.g. 0.39–0.47°Brix by McGlone and Kawano, 1998). However, these data were derived using *Actinidia deliciosa* and over a smaller range of SSC than that reported here with *A. chinensis*.

The corresponding values of R^2_P reported by McGlone and Kawano are lower (0.90–0.85) than the value we found (0.93).

The SEP for the flesh hue angle calibrations, listed in Table 4, were between 1.6 and 2.0°. The replicate flesh hue angle measurements presented in Fig. 3(c) suggest that within-fruit variability in calibration measurements of hue angle is approximately 1.3°, suggesting that errors in the calibration data may comprise a significant component of the SEP.

The 'comet-like' distributions for hue angle calibrations shown in Fig. 8 result from the combination of a relatively high number of mature fruit with low hue angle, evident in Fig. 2, and calibration errors which increase with hue angle, shown in Fig. 3(c). The reflectance mode calibration for hue angle, graphed in Fig. 8, shows a clear non-linear trend, suggesting the need for further, non-linear, spectral pre-processing.

5. Conclusion

This study compared the relative accuracy of reflectance, transmission and interactance modes of NIR spectroscopy for estimating SSC, density and flesh hue of *Actinidia chinensis*, and evaluated the optimal method for deriving the calibration. Good calibrations were obtained in every case, supporting the use of NIR spectroscopy for the rapid and non-destructive evaluation of fruit internal qualities. In each case the most accurate results were obtained using interactance mode, followed by transmission mode, and in general reflectance was least accurate. PLS proved to be the most robust algorithm of those tested for generating calibration models.

Acknowledgements

This work was funded by Kiwifruit New Zealand and by the New Zealand Foundation for Research, Science and Technology. Thanks to our colleagues Bob Jordan and Andrew McGlone in the Technology Development Group for many helpful discussions and to Alan Harris, Annette Richardson and Philip Martin for their assistance.

References

Abbott, J., Lu, R., Upchurch, B., Stroshine, R., 1997. Technologies for nondestructive quality evaluation. Hort. Rev. 20, 1–120.

Asami, I., Tanaka, Y., Aoki, M., 1988. Studies on the quality evaluation of kiwifruit. (I) Chemical composition and a non-destructive quality evaluation method for kiwifruit. Res. Bul. Aichi ken Agr. Res. Ctr. 20, 309–316.

Barnes, R.J, Dhanoa, M.S., Lister, S.J., 1989. Standard normal variate transformation and de-trending of near-infrared diffuse reflectance spectra. Appl. Spectrosc. 43, 772–777.

Bellon, V., Vigneau, J.L., Leclercq, M., 1993. Feasibility and performances of a new, multiplexed, fast and low-cost spectrometer for the on-line measurement of sugars in fruit. Appl. Spectrosc. 47, 1079–1083.

Dull, G.G., Birth, G.S., Smittle, D.A., et al., 1989. Near infrared analysis of soluble solids in intact cantaloupe. J. Food Sci. 54, 393–395.

Fearn, T., 1996. Comparing standard deviations. NIR News 7 (5), 5–6.

Geladi, P., MacDougall, D., Martens, H., 1985. Linearization and scatter correction for near-infrared reflectance spectra of meat. Appl. Spectrosc. 39, 491–500.

Greensil, C.V., Newman, D.S., 1999. An investigation into the determination of the maturity of pawpaws (*Carica papaya*) from NIR transmission spectra. J. Near Infrared Spectrosc. 7, 109–116.

Jordan, R.B., Osborne, S.D., Kunnemeyer, R., Seelye, R.J., 1997. Harvest time prediction of eating time properties of kiwifruit using NIR transmission, Proceedings of the Sens. Nondestr. Sens. Test. Int. Conf., Northeast Reg. Agric. Eng. Serv., Ithaca, New York, pp. 101–110.

Kawano, S., 1994. Present condition of nondestructive quality evaluation of fruits and vegetables in Japan. Jpn. Agric. Res. Q 28, 212–216.

Kawano, S., Watanabe, H., Iwamoto, M., 1992. Determination of sugar content in intact peaches by near infrared spectroscopy with fiber optics in interactance mode. J. Jpn. Soc. Hort. Sci. 61, 445–451.

Kawano, S., Fujiwara, T., Iwamoto, M., 1993. Nondestructive determination of sugar content in Satsuma mandarin using near infrared (NIR) transmittance. J. Jpn. Soc. Hort. Sci. 62, 470–645.

McGlone, V.A., Kawano, S., 1998. Firmness, dry-matter and soluble-solids assessment of postharvest kiwifruit by NIR spectroscopy. Postharvest Biol. Technol. 13, 131–141.

Miyamoto, K., Yoshinobu, K., 1995. Non-destructive determination of sugar content in satsuma mandarin fruit by near infrared transmittance spectroscopy. J. Near Infrared Spectrosc. 3, 227–237.

Miyamoto, K., Kuwauchi, M., Fukuda, T., 1997. Classification of high acid fruits by partial least squares using the near infrared transmittance spectra of intact satsuma mandarins. J. Near Infrared Spectrosc. 6, 267–271.

Mowat, A.D., Poole, P.R., 1997. Use of visible-near infrared diffuse reflectance spectroscopy to discriminate between kiwifruit with properties altered by preharvest treatments. J. Near Infrared Spectrosc. 5, 113–122.

Norris, K.H., Workman, J. Jr, 1997. NIR News 8 (4), 7.

Osborne, S.D., Jordan, R.B., Kunnemeyer, R., 1998. Using near infrared (NIR) light to estimate the soluble solids and dry matter content of kiwifruit. Acta Hort. 464, 109–114.

Schmilovitch, Z., Ben-Zvi, R., Hoffman, A., Bernstein, Z., Egozi, H., Alchanatis, V., 1997. System and method for pre-harvested maturity determination of fresh dates by near infrared spectrometery, Proceedings of the Sens. Nondestr. Sens. Test. Int. Conf., Northeast Reg. Agric. Eng. Serv., Ithaca, New York, pp. 111–121.